International Journal Of Engineering Research And Development
e- ISSN: 2278-067X, p-ISSN: 2278-800X, www.ijerd.com
Volume 17, Issue 2 (February 2021), PP. 09-18

Dynamic Simulation of the Chain Drive in a Vertical Stereo Garage on Adams Software.

Chen Qinghua[1], Melangi Momo Valex[2]
[1]*Anhui key Laboratory of Mine Intelligent Equipment and Technology, Huainan 232001, China*
[2]*College of Mechanical Engineering, Anhui University of Science and Technology, Huainan, China.*

Abstract
The vertical stereo garage is a smart car parking system. Parking is achieved through a chain drive which enables parking slots to be rotated. The aim of this paper is to simulate the dynamics of this chain and provide a base for its optimization. A chain model is built on ADAMS software and analyzed. Torques corresponding to the loads of cars is applied to each sprocket. Forces in the chain are investigated. Results show that applied torques remain constant throughout the experiment. Graphs of contact and tension forces are in phase. Moreover the maximum value of the average tension force is compared with the standard average tensile strength of the 48A chain, revealing a safety margin of 75.75%.
Keywords: *Contact, tension, chain drive, dynamic simulation*.

Date of Submission: 11-03-2021 Date of Acceptance: 26-03-2021

I. Introduction

The world population is rapidly increasing[1] with time. More people own cars, consequently the problem of parking prevails[2]. The car industry is fast evolving with the population growth to meet the society's transportation demands. According to a quote on Parking Industry Development, the ratio of cars to parking space in China is 2:1, and the parking sector should be worth 17 trillion Yuan ($2.55 trillion) to meet most of the needs [3]. The vertical stereo circulation is chosen as a remedy to this problem. The roller chain being a major assembly of this system is studied in order to provide a better transmission. So far there have been a number of articles on dynamic simulations of chains, that apply to different machines but very few articles focus on the dynamic simulation of the chain drive of this garage. Wang Xue et al studied the stress deformation of a heavy scraper conveyor during starting load, due to the contact forces at the nodes[4]. Also, a different paper still on the dynamics analysis of a scraper conveyor[5] was done but this time, based on Amesim. A Vogit model was used here to cover the lapses of the pressure applied on the chain in previous models. According to this model, the tension is applied while the pressure is not. Notwithstanding, the paper highlights a significant polygon effect due to the speed and tension fluctuation of the chain. Furthermore, in the simulation of a double scraper chain by the China Coal Science and Technology group Taiyuan research Institute Company, the dynamics of the chain was simulated using cero 2.0 software, instead of Adams like other models [6]. In another piece of writing, the author modifies the profile of the tooth sprocket in order to reduce the polygon effect and the vibration in the chain [7]. The author created a new tooth profile on SOLIDWORKS and later used ADAMS to apply forces on the generated model. The results showed that the amplitude of the upward and downward vibration of the chain was reduced from 2.35mm to 1.595mm at the crest. Another article equally improved on the polygon effect of a roller chain [8]. At the Nanjing University of Science and Technology, the dynamics of the chain transmission of a ramming mechanism was studied [9]. The contact forces between the sprocket and the chain were monitored and analyzed. Results proved that the clearance between the sprocket and the chain has an impact on the dynamic characteristics of the chain drive and should be carefully chosen. Different writers used a generalized revolute clearance method [10], which was mainly based on the geometry of the tooth profile. Some went deeper in building an experimental device to study the vibration in the chain motion[11]. In addition an experimental investigation was done in an automotive bush chain drive to monitor the internal friction. Here parameters like engine speed and engine oil were focused on.

During the modelling and simulation of a large diesel engine on ADAMS [12], it was shown that the contact forces varied at each point on the sprocket, from a maximum to zero, where there was no contact with the sprocket. The dynamic model established here was close to that of our case study. Mulik et al equally studied the timing chain system in a diesel engine[13] and got results expressed in tension forces, whose values at the end of simulations were below maximum permissible values. Also, another paper on chain drive dynamic simulation of an Apron feeder [14] suggests that the pitch and number of sprockets greatly influence the impulsive loads that affect the chain. This paper lays emphasis on the relationship between design parameters and the speed fluctuation of roller chain whereas previous papers mostly dealt with contact forces and not design parameters. In the roller chain dynamic analysis of heavy duty ship unloader [15], the authors varied the speed of the chain, to show that the vibration had to be considered in the design as well as contact and tension forces. RecurDyn was used by other authors for the chain dynamic simulation, like the case of Juntian Zhao et al [16]. It provides a different approach to analysis via the recursion theory. This theory organizes the algorithm structure of constraint equations of motion and classifies them in a recursive fashion. An article on the kinematic and dynamic analysis of a roller chain drive [17] contributed to providing a framework to understanding both numerical and experimental investigations on the chain drive. Multi-body dynamics was used in another simulation of a conveyor chain drive system, where average error results of 3.95%[18].

1.1. Overview of the vertical stereo circulation garage

The vertical stereo circulation garage is a three dimensional structure which aims at parking cars easily, accurately, quickly and safely at the same time, saving ground parking area. So far this system is been used in many cities in China and it gradually spreads to other parts of the world like Japan, Germany and United States of America. The number of vehicles accommodated by this system varies depending on the user. For our case study, we use 12 cars. This parking space of 4900 × 2500 × 1800 mm (length, width and height respectively) was designed to support 2000kg for each space.

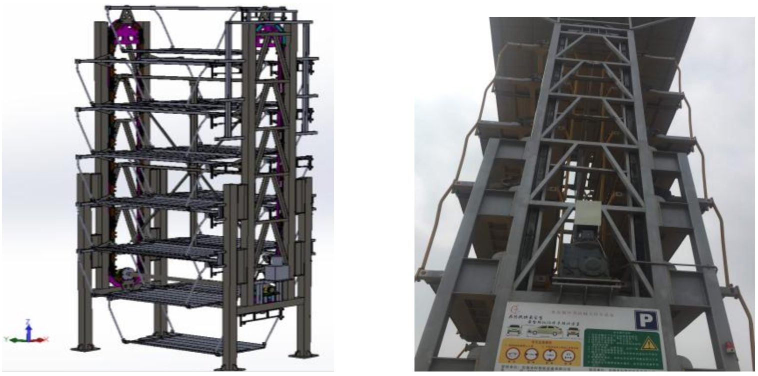

Figure 1: 3D Structure of the vertical stereo circulation garage.

The Sedan is supported at the bottom by a thin sheet of steel material, connected at the four edges by bolts, to the upper steel rods. The mid-upper rod is in turn linked to the thin plates through perpendicular rods on which ball bearings are attached at both ends. The ball bearings permit free rotation so that the sedan always stays in a horizontal position while the chain transmits the motion from the gear box and electric motor. The ball bearings also mesh in a guide to prevent lateral movement of the sedan during operation. The different linking plates are designed in a close circular loop, to assist in giving smooth direction to the rotating sedan. Describing this motion in the reverse direction, the non-standard sprocket connected to the link plates, which in turn is connected to the large sprocket, chain and small sprocket. All these are linked by a shaft of diameter 0.2m.

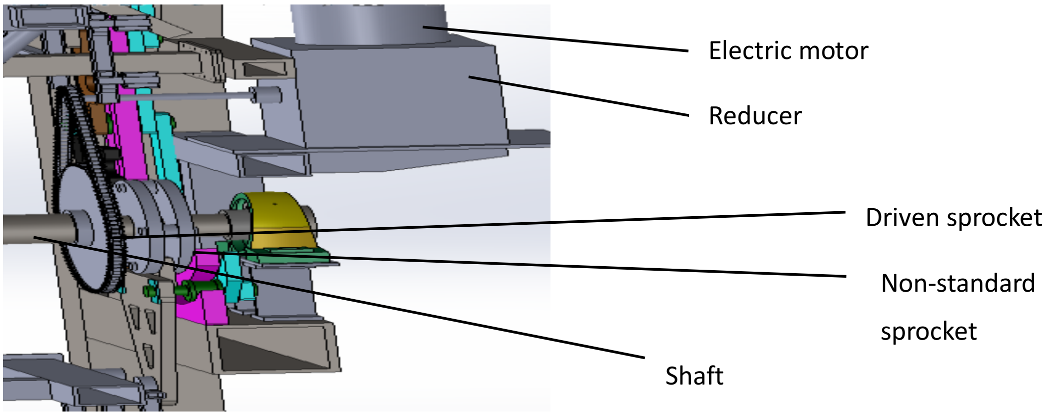

Figure 2: Driving system of the garage

The electric motor which drives the system has a capacity of 22KW, but the actual power needed is 15KW. The speed is set at 6m/min. One car is packed at a time. The structure is capable of rotating clockwise or anticlockwise depending on the position of the requested packing space. A PLC controller is used to manage the electric commands[19].

Figure 3: Actual chain system at the garage

II. MATERIALS AND METHODS

2.1 Model

Let *V* be the vector from one roller to another;

$V_{i-1} = V_{i-1} - V_i$ (1)

$V_i = r_i - r_{i-1}$ (2)

$V_{i+1} = r_{i+1} - r_i$ (3)

Where: *i* represents the roller; r = position vector from the frame to the center of the roller; r = (xr, yr) - position vector with respect to the frame

From newton's law, $F = Ma$ (4)

Hence $[M_r][\ddot{x}, \ddot{Y}] = [F_{xn}, F_{yn} - mg]$ (5)

Where: g = gravity in the negative y-direction; n = number of links; Fx = resultant force of roller V in the x-direction; Fy = resultant force of roller V in the y-direction.

Since the elements are considered as mass properties, in the y- direction the force of gravity acts in a direction opposite to the frame. Hence the force in the y-direction is $F_{yn} - mg$. Considering only the x-component, equation (5) becomes

$[M_r][\ddot{x}] = [F_{xn}]$ (6)

The illustration is shown figure 1 below:

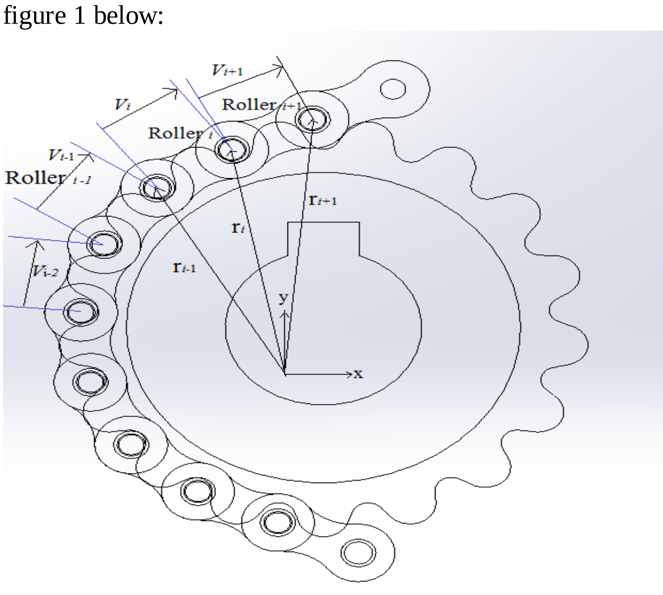

Figure 3: dynamic model of the chain and driver sprocket

The dynamics of the roller chain is studied in ADAMS software. The chain and sprockets are generated on the software and simulated. A clockwise torque from the motor is applied to the small sprocket and the loads on the sedan equivalent to the number of cars are converted to another torque, which is applied anticlockwise to the large sprocket.

2.2. Geometry

The small sprocket consists of 21 teeth, while the large sprocket consists of 57 teeth. The software automatically generates the number of links to be 76 links. It equally calculates the tension in the chain. We then run several simulations while altering the number of cars packed by varying the resulting torque, with the same number of chain links in order to investigate the contact forces and tension forces during the transmission. Figure 2 below illustrates the built model on ADAMS.

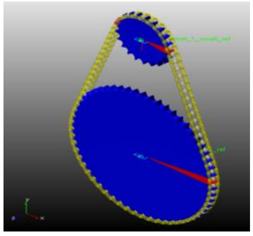

Figure 4: Chain and sprocket model generated on ADAMS

The units where set to standard m, kg, N as well as the working grid. The first step was to generate sprockets for the transmission. Roller sprockets and 3D links were chosen as method. Then the parameters of the input and output sprockets were entered as follows [20]

Parameter	Driver sprocket	Driven sprocket
Center location	0,0,0	0,-1.33841,0
Sprocket width	0.04	0.04
Number of teeth	21	57
Pitch diameter	0.51	1.38
Root diameter	0.47	1.35
Seat radius	0.02	0.02
Tip diameter	0.55	1.43

Table 1: driver and driven sprockets parameters.

For each set of simulation, the torque was altered (from 20436.39Nm to 122618Nm as shown in table 2), while maintaining the same basic parameters shown above in table 1. Next, the materials were set as mass property with inertia and the sprockets were connected as rotational elements. Finally the output sprocket's motion was computed for angular displacement, angular velocity, angular acceleration and joint force.

The next phase was to create the chain from the generated input and output sprockets. Also, 2D links were used with a linear compliance for easy and fast simulation. The linear compliance method was chosen because the links are along the main axis of the chain. The geometry of the chain included the chain pitch which was 0.0762m, the chain width chosen as 0.0955m, pitch to back 0.07239m and roller diameter chosen as 0.0238m, from reference [14]. This chain was earlier designed for this purpose, and the parameters listed above were inputted into ADAMS. The translational stiffness and damping were 1.008E+005 and 10.08 respectively. The rotational damping was 0.1. On the chain geometry, simple links were used in order to better view the rollers' positions in the course of the simulation. The mass properties were set and the chain was automatically wrapped by the software. For each set of simulation where by the torque was different, the number of links remained un-changed.

In addition to the chain wrap, the actuator was set. This is the phase where the driving motion is selected. The chain system was selected and the torque value for the driving sprocket was set as a constant 76689Nm, in an anti-clockwise direction. All these being successful, the simulation ran for 2 seconds, with 100 steps.

2.3. Torque calculation

The motor delivers a power of 15kW, and the chain is expected to run at 6m/min (equivalent to 0.1m/s). The anticlockwise torque at the driver sprocket is calculated from the input power of the motor. The reducer is assumed to have 100% efficiency, which implies that the same power will be transmitted to the sprocket. Likewise, the load of the vehicles (2000kg per car) is converted to a torque, which is applied to the driven sprocket in a clockwise direction so as to oppose the driving torque. As such, during the simulations different torque values are used for each simulation, corresponding to the number of cars loaded. It should be noted that the only six cars out of the 12 are required to be lifted, because the other cars move downwards under the influence of gravity force. Hence, 6 sets of simulations are carried out, corresponding to six cars.

2.3.1. Anti-clockwise driving torque

$$P = FV$$

$$F = \frac{P}{V} \qquad (7)$$

$$= \frac{15\ kW}{6\ m\ /\ \min}$$

$$= 150000\ N$$

$$T = F \times L \qquad (8)$$

$$= 150000\ N \times 0.51126\ m$$

$$= 76689\ Nm$$

Where: P = Input power(W), F = Force(N), V = velocity(m/s), T = torque, L = distance from the point of action to the torque (radius of the sprocket)

2.3.2. Clockwise torque

$$T = F \times L$$

$$= m \times a \times L$$

$$= 2000\ (6) \times 9.81 \times 1.04161$$

$$= 122618\ .33\ Nm$$

Above is the torque for 6 cars. The same procedure is repeated for the other 5 vehicles by simply multiplying by the number of cars as shown in table 2 below

Number of cars	Torque (Nm)
6	122618.33
5	102181.94
4	81745.55
3	61309.16
2	40872.78
1	20436.39

Table 2: Torque used during simulations

III. RESULTS AND DISCUSSION

3.1 Results

Below the the output graphs of contact and tension forces for the same link (link 1 with ADAMS Id 153), during the six different simulations.

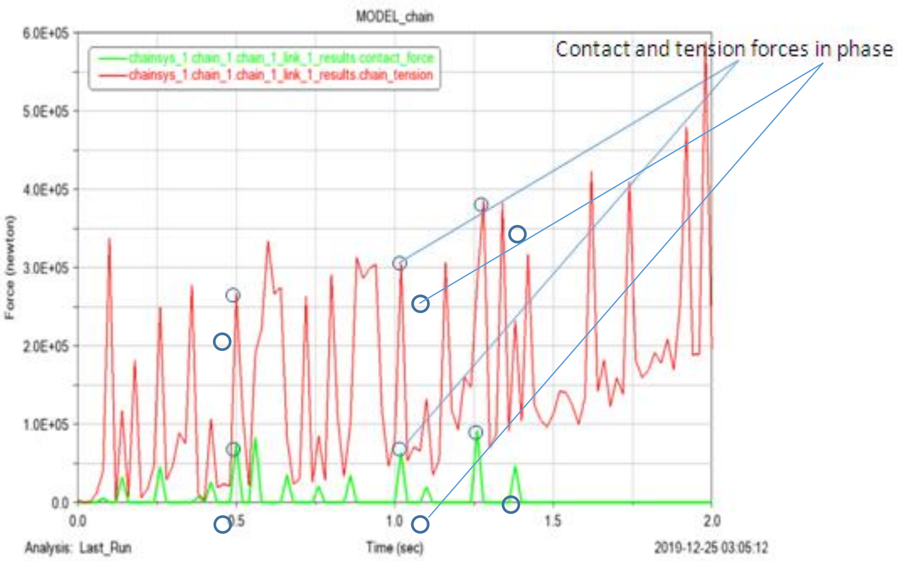

Figure 5: Contact and tension forces at link 1 for one car load

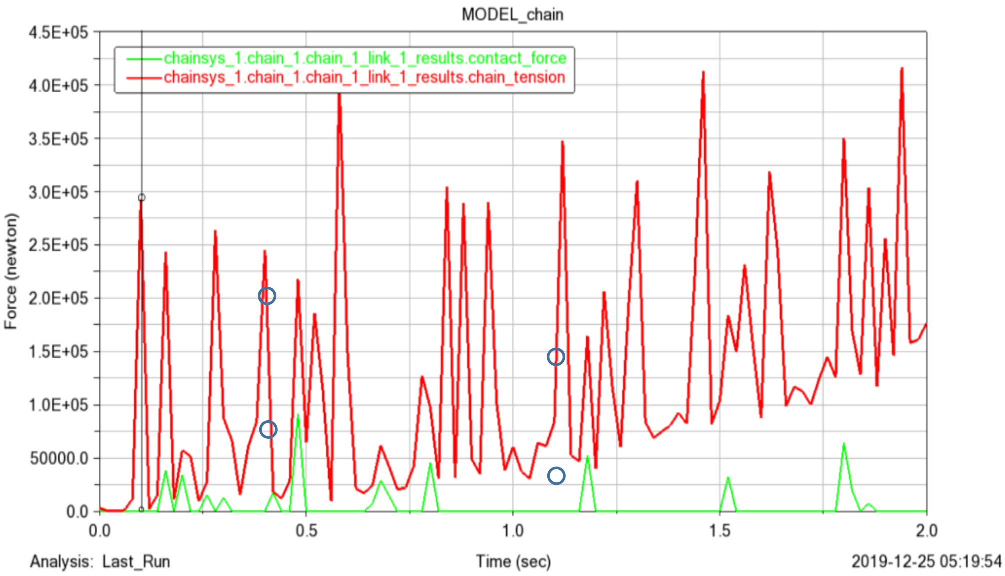

Figure 6: Contact and tension forces at link 1 for two cars load

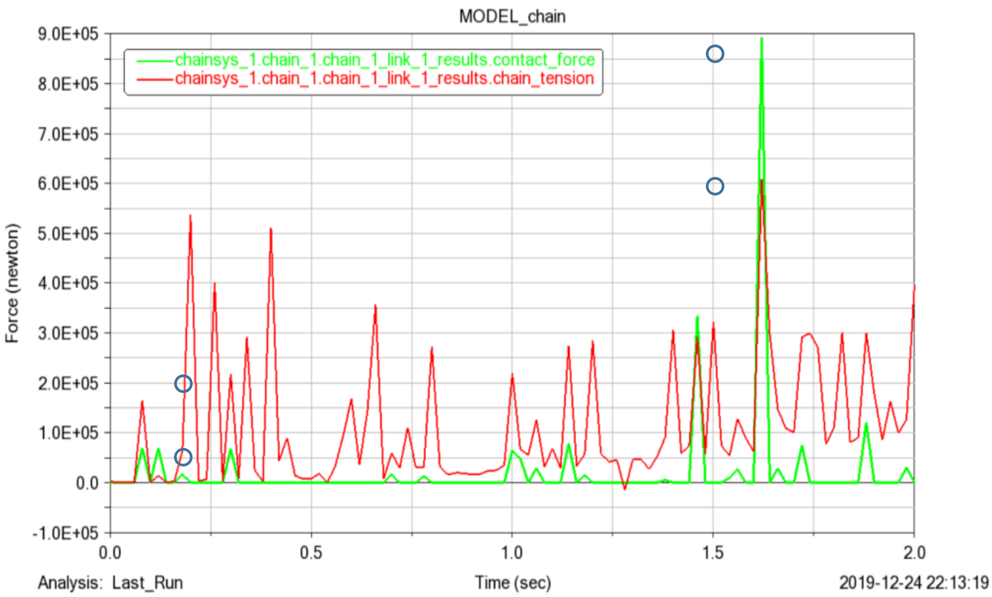

Figure 7: Contact and tension forces at link 1 for three cars load

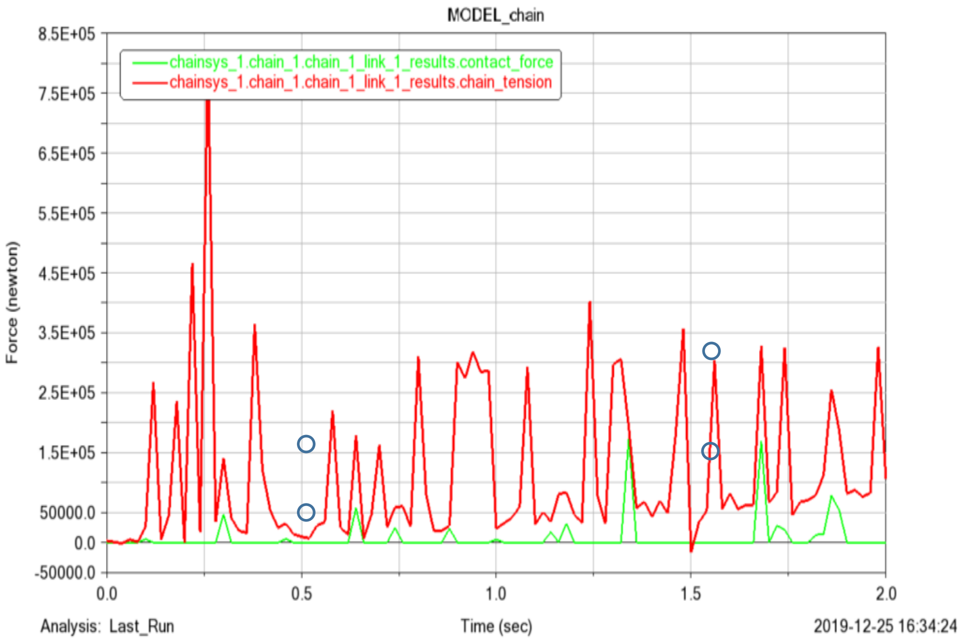

Figure 8: Contact and tension forces at link 1 for four cars load

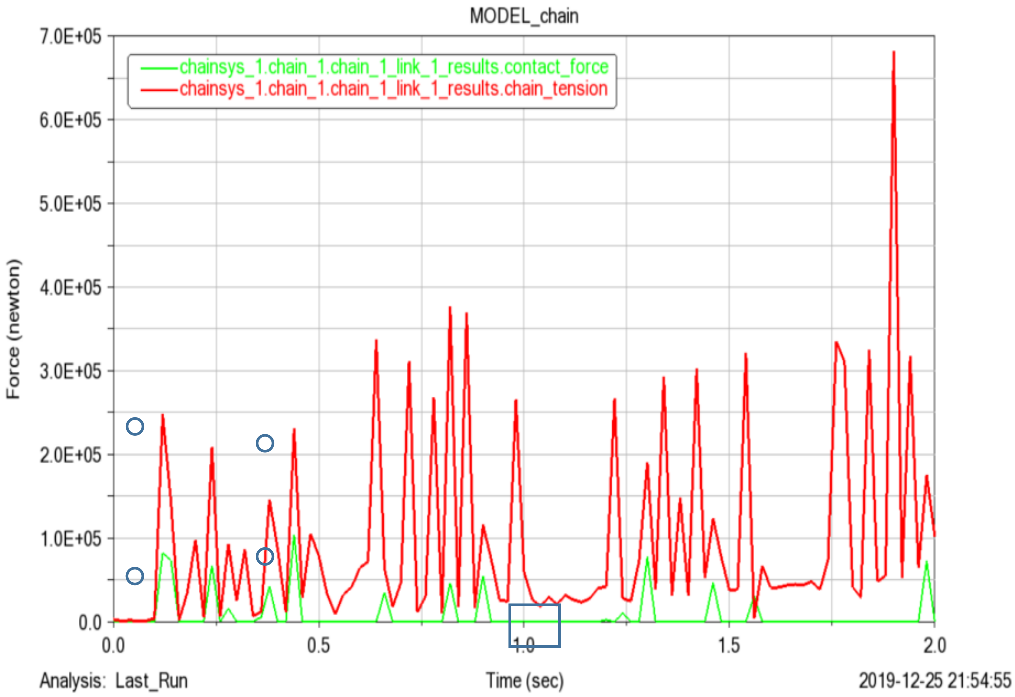

Figure 9: Contact and tension forces at link 1 for five cars load

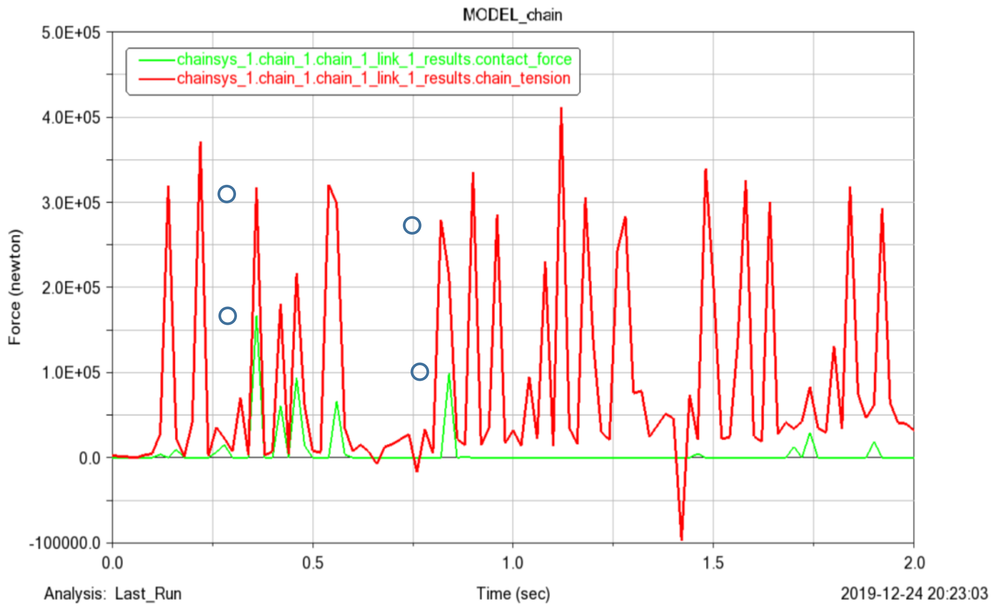

Figure 10: Contact and tension forces at link 1 for six cars load

Table 3 shows the average contact and tension forces for the six different simulations, corresponding to the torques the number of cars packed.

Number of cars	Contact forces/N	Tension forces/N
1	5892.68	150960
2	4768.18	120430
3	19953.93	112120
4	7671.28	114840
5	7623.46	96311
6	6032.27	86722

Table 3: Average contact and tension forces of the six simulations for link 1

The average tension and contact forces in each of the simulations where compared with respect to the reference and represented on the graphs in figure 11 below.

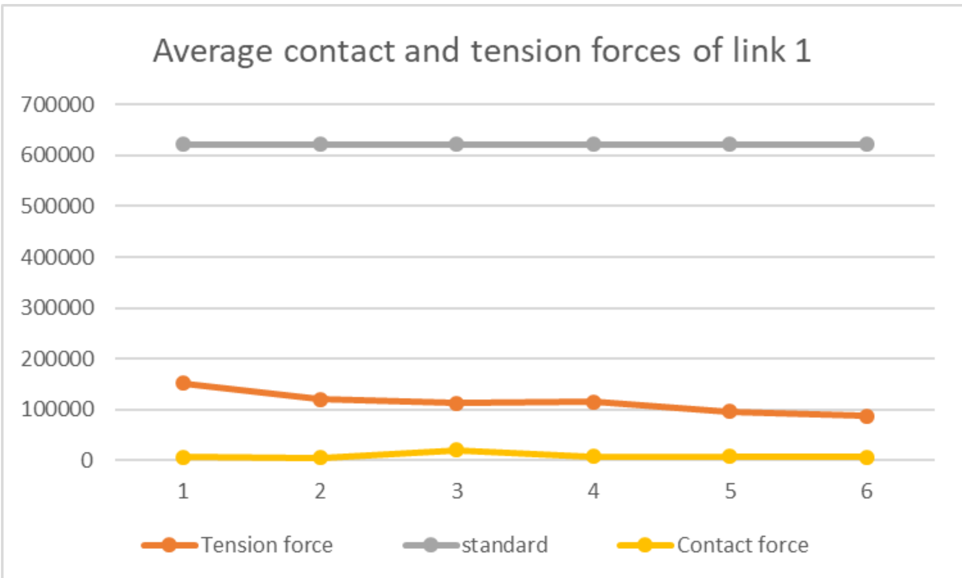

Figure 11: The average contact and tension forces compared with the reference tensile strength.

The representation of the torque curves generated by ADAMS software after the simulation is viewed in figure 12 below.

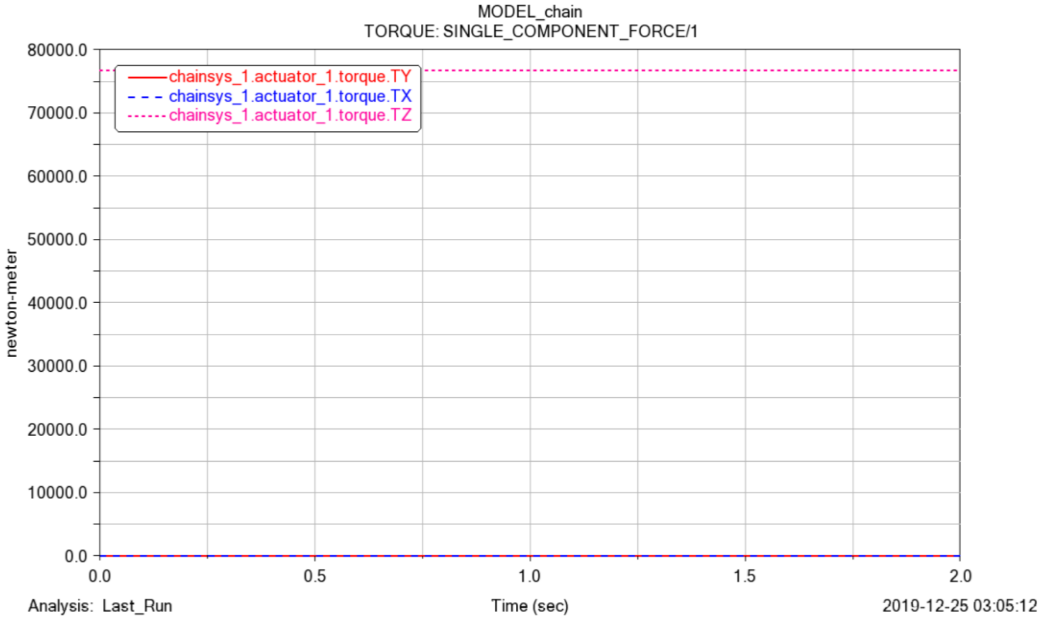

Figure 12: Result set for torques applied, showing a constant driving torque along the Z direction and a zero torque along both X and Y directions.

3.2 Discussion

The contact and tension forces of each simulation were overlapped for analysis as seen from figure 5 to figure 10. Link 1 was taken as reference throughout the process. The peak values of these individual graphs vary haphazardly from the least to the highest load. Nevertheless these peaks and crests of contact and tension forces highlighted in blue are in phase. That is, an increase in the contact force is marked by a corresponding increase in the tension force at that time, as seen in figure 5 at t=1s. Similarly when there is less contact on the chain, the tension force is low. For example, the highlighted region in figure 9 between 1s and 1.25s. This general tendency of contact and tension forces aligning is observed throughout the experiment. Higher tension forces occur when there are corresponding higher contact forces and vice-verse hereby proving the consistency in the results from the applied torques.

In addition, different values for average tension forces and contact forces were noted from the various simulations of link 1 as summarized earlier in table 3. These average contact and tension forces were automatically calculated by the software ADAMS. The ‘number of cars’ were simulated separately to represent the load moved by the chain. The average tensile strength of this 48A chain as per the reference[21] is 622500N. Tensile strength is the maximum stress the chain can withstand before failure. Figure 11 further illustrates the average tension and contact forces. The contact forces are smaller, compared to the tension forces (the contact force curve is beneath the tension force curve). The difference between the average contact force and the average tension force is significant as shown in figure 11 by the gap between the curves. The difference between the average contact and tension forces curves with the reference is equally very big. This gap represents the safety range in which the chain operates. We can hence make analysis with the tension force curve while using the contact force curve as a guidance to monitor the evolution of the simulations.

The general trend of the tension curves are decreasing from 150960N to 86722N. The tension forces decrease with an increase in the number of cars because the input torque is kept constant, while the driving sprocket is smaller in diameter than the driven sprocket, hence when the car loads (converted to torques on the driven sprocket) are applied on the larger driven sprocket, the tension forces tend to reduce from a maximum value with one car to a minimum value with six cars. The resultant torque is in the direction of the input torque, but to the load of the larger size driven sprocket slows down the number of revolutions of this sprocket, hence reducing the tension value.

The highest value from table 3 is 150960N which confirms that the chain is operated within a wide range of safety, compared to 622500N. From this comparison the safety range is 75.75%, which can be considered as a successful outcome.

The result set for the constant input torque applied is equally collected after the simulation, and shows that this applied torque in the z direction remained constant throughout the simulation while neither torque nor force was applied in the other directions to influence the results. This is clearly illustrated in figure 12 with the constant input torque of 76689N about the Z axis, represented by a straight horizontal line. The other torques about the X and Y axis are equally represented by a constant straight line with value 0.0 N each.

As per the analysis done on the dynamic simulation on reference [7], it was concluded that the clearance between the rollers should be well monitored during design. Also, during this experiment [7] a fluctuation in the contact force was noticed as the gap increased. In the same line, altering the number of cars in our experiment brings about a change in the tension and contact forces in the chain.

IV. CONCLUSION

Taking the chain drive of the 3D vertical stereo circulation garage as subject, the generated and simulated 76.2mm pitch chain on ADAMS Machinery was successful. The results showed encouraging tendencies of tension and contact forces values in accordance with the references. Hence, this simulation can be used as a reference to monitor the tension and contact forces, for better and safer chain drive operations. This method of converting forces to torques before application is more convenient saves time and efficient because the exact torque is applied directly to the sprockets. The transmission is smooth but further studies could be done to reduce the polygon effect using this method.

ACKNOWLEDGEMENT

We acknowledge Eileen Goody Gans-Lartey for her endless efforts invested in this article.
This research did not receive any specific grant from funding agencies in the public, commercial, or not-for-profit sectors.

REFERENCES

[1]. Trupti Y. Nirwan, Akash S. Waghmare, Gaurav R. Rahate, Kartik Bhujade, Asaraf Ali Saiyyad, Adarsh Shahu, Prof. A.D. Anjikar. Introduction to vertical multistage car parking system. International Research Journal of Engineering and Technology (IRJET)Volume: 03 Issue: 04 | Apr-2016.

[2]. Chandni Patel, Monalisa Swami, Priya Saxena, Sejal Shah. Rotary Automated Car Parking System. ISSN: 2319-5967.ISO 9001:2008 Certified.

[3]. China Daily. Shared parking app needs policy support: August 21, 2017. Reference to a website: http://www.china.org.cn/opinion/2017-08/21/content_41445971.htm. Last visited 2019/05/31.

[4]. WANG Xue, WANG Shu, LONG Ri Sheng, Yang Zhao Jian, Liu Guang. PengRigid flexible coupled dynamic contact analysis of a chain drive system of a heavy scraper conveyor during loading start up. Shanxi Key Laboratory of Fully Mechanized Coal Mining Equipment, Taiyuan University of Technology. Journal of vibration and shock vol 35 No 11, 2016

[5]. Yanqing Hu, Qingliang Zeg, Shoubo Jiang, Pengfei Yu and Zhikuan Yang. Dynamic analysis of chain Drive System for Scraper Conveyor Based on Amesim. College of Mechanical and Electronic Engineering Shandong university of Science and Technology Qingdao, China 2018.

[6]. China Coal Science and Technology group Taiyuan research institute company. Dynamic Simulation of a double scraper chain with sleeve roller slide under multiple working conditions, 2015.

[7]. Xue Yunna, Wang Yong, Wang Xianlun. Profile modification and dynamic simulation of sprockets silent chain, 2006.

[8]. Yong Wang, Deshebg Ji, Kai Zhan. Modified sprocket tooth profile of roller chain drives. school of mechanicl Engineering, Shandong University, Jin-Shi Road 17923, Jinan 250061, China; Key laboratory of High-efficiency and clean Mechanical Manufacture (Shandong university), Ministry of Education, China.

[9]. LiU Tai-su, QIAN Lin-fang, CHEN Guang-song, JI Lei. Dynamics modeling Analysis of open Chain Drive Transmission for a Ramming mechanism. School of mechanical engineering, Nanjing University of Science and Technology, vol 39.No 11.Nov 2018.

[10]. C. Pereira, J. Ambrosio, A. Ramalho. Dynamics of Chain drives using a generalized revolute clearance joint formulation. Polytechnic instistute of Coimbra, R Pedro Nunes, 3030-199 Coimbra, Portugal.

[11]. Li-Xin Xu et al. Clearance influence on dynamic response of intermittent roller chain drive. Chinese journal of mechanical engineering: June 2010.

[12]. Su Yang, Zhou Ruiping, Wang Zhengxing, Gan Shaojing. Modeling Method and Dynamics Simulation Analysis about Roller Chain Drive System of Large Diesel Engine (Wuhan University of technology, 430063): 2017.

[13]. R.V. Mulik, Prof.M.M. Joshi et al. Dynamic analysis of timing chain system of a high speed three cylinder diesel engine. International journal of engineering and science vol 4, issue 5 (May 2014) PP 21-25]

[14]. Junzhou Huo, Shiqiang Yu, Jing Yang and Tao Li. Static and Dynamic Characteristics of the Chain Drive System of a Heavy Duty Apron Feeder. School of Mechanical Engineering, Dalian University of Technology, Dalian, 116023, China. The Open Mechanical Engineering Journal: 2013, 7, 121-128.

[15]. Chang-Uk Jim, Jang- Young Chung, Jung-II Song. Dynamic analysis of a long heavy duty roller chain for bucket elevator for continuous ship unloader. Advances in Mechanical Engineering: 2017 Vol 9(8) 1-11.

[16]. Juntian Zhao, Shunzeng Wang, Shengyang Hu, Yu Liu. Dynamic Analysis and simulation of a roller chain drive system based on RecurDyn: 2014.

[17]. N.Fuglede et al. Kinematic and dynamic modelling and approximate analysis of a roller chain drive. Depatement of mechanical engineering, Technical University of Denmark, Building 404 DK-2800 Lyngby, Denmark: 2015

[18]. Chakrit Suvanjumrat et al. Implementation of multi-body dynamics simulation for the conveyor chain drive system: 2017.

[19]. Chandni Patel, Monalisa Swami, Priya Saxema, sejal shah. Rotatory Automated car parking system. International journal of Engineering Science and innovative technology: volume 4 issue march 2015.

[20]. Cheng Da Xian, Wang De Fu et al. Handbook of mechanical design 3. ISBN 7-5025-3521-7. Pg 13-101. 2001.

[21]. Power Transmission solutions NIS catalogue: Cat 03-01 (P2008) last accessed March 2020.